inventions

Article

Conveyor-Belt Dryers with Tangential Flow for Food Drying: Development of Drying ODEs Useful to Design and Process Adjustment

Dario Friso

Department of Land, Environment, Agriculture and Forestry, University of Padova, Viale dell'Università 16, Agripolis, 35020 Legnaro, Italy; dario.friso@unipd.it

Abstract: The mathematical investigation presented in this paper concerns the conveyor-belt dryer with tangential flow operating in co-current. This dryer is bigger than the continuous through-circulation conveyor dryer but has the advantage of better preserving the organoleptic and nutritional qualities of the dried product. In a previous work a mathematical modeling of the conveyor-belt dryer with tangential flow was carried out to offer guidelines for its optimized design. The last of those design guidelines indicated the need for an optimized adjustment of the dryer to ensure the constant maintenance of the final moisture content of the product. The fast and very precise measurement of the moisture content as the first step in the feedback chain was therefore necessary. Considering the difficulty of this type of measurement, two specific ordinary differential equations (ODEs) were obtained with the mathematical investigation of this work. Their solution became a relationship between the final moisture content of the product, the outlet air temperature, and other quantities that could be easily implemented in an automatic dryer control system. Therefore, the fast and accurate and much less expensive measurement of the temperature of the air leaving the dryer, owing to the relationship found, replaces the measurement of moisture content for the adjustment system. The experimental verification of the relationship highlighted the need to introduce a modification by which the relationship was finally validated.

Keywords: conveyor-belt dryer; food drying; mathematical modeling; design; food quality; food safety; dryer adjustment

check for updates

Citation: Friso, D. Conveyor-Belt Dryers with Tangential Flow for Food Drying: Development of Drying ODEs Useful to Design and Process Adjustment. *Inventions* **2021**, *6*, 6. https://doi.org/10.3390/inventions6010006

Received: 8 November 2020
Accepted: 7 January 2021
Published: 11 January 2021

1. Introduction

Food products are dried to reduce water activity [1,2] within safe limits. In this way, food can be stored at room temperature, reducing storage costs [3–6].

The contact of the product with hot and dry air leads to an increase in temperature with the risk of loss of nutritional qualities [7,8]. However, this loss of quality is acceptable because during drying, the product assumes the wet bulb temperature which is much lower than the dry bulb temperature of the air. For example, if this is 120 °C, the wet bulb temperature is about 38 °C as shown in a psychrometric chart. This phenomenon is possible if the product remains above the critical moisture content X_C until the end of dryer where the moisture content is X_F. This is an assumption imposed in this work, that is $X_F > X_C$.

During drying, between the air and the product there is a heat and mass exchange described by differential equations [9,10]. These equations can be solved in closed form [11–13] or with numerical methods. Many results have emerged from these mathematical modeling over several decades. They were then applied to a multitude of products: madarin [14], apple [15–19], apricot [20], mango [21–24], coroba [25], pear [26], kiwi [27], papaya [28], coconut [29], sultanas [30], banana [31–33], generic fruits [34–39], generic foods [40–53].

The mathematical modeling of the operation of dryers and therefore the definition of guidelines for their design has also been the subject of study in the past and continues to be so today.

Among the many types of dryers for food products [54,55] perforated belt dryers are quite frequent, because of their small size. However, they, which have been the subject of various studies [56–62], present the problem of a high air temperature even in the final area of the dryer where the food product is more thermosensitive.

In a previous work [63] a conveyor-belt dryer with tangential flow was studied (Figure 1). This dryer has a lower air temperature in the terminal area of drying thus allowing greater respect for the product, with reduced denaturation of proteins and of polyphenols. The lower temperature at the end of this dryer results in a longer drying time, but being a continuous dryer, it results in an increase in its length.

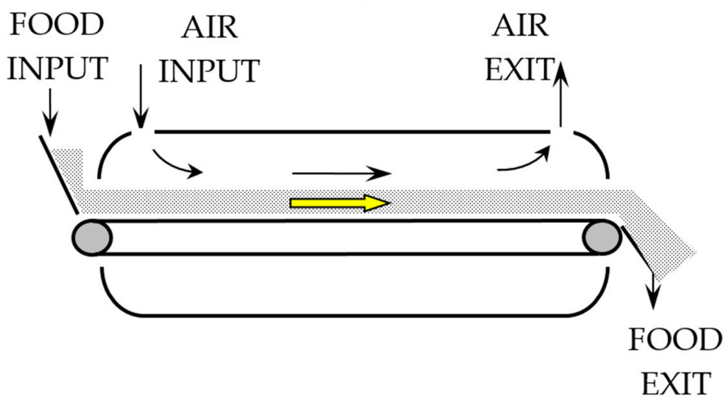

Figure 1. Conveyor belt dryer with tangential flow in co-current.

Its operation is shown in Figure 1 where a unperforated belt carries the product which is lapped by the air in co-current. Therefore, the air has a continuous variation of its characteristics of temperature T_A and humidity x, along the dryer and this required a special mathematical modeling developed in the previous work [63], under the condition that the final moisture content of the product was higher than the critical one ($X_F > X_C$).

As result of the mathematical model, among the design guidelines proposed by [63], the last one concerned adjustment with the dryer feedback system. The mathematical model had indicated, for the feedback control chain, the need to start from an instant measurement of the final moisture content of the product.

The instantaneous measurement of moisture content requires using the dielectric properties of the product and the results obtained with such capacitive instruments, when applied in line on fast flowing product can be undermined by important measurement errors. To try to overcome this problem, in this work a mathematical analysis is carried out to develop two ordinary differential equations (ODEs) of drying for these specific dryers. The solution of the ODEs will allow to find a relationship between some quantities including: the moisture content of the initial and final product and the dryer input and exit air temperatures. Therefore, a relationship exists between the final moisture content of the product and the air temperature at the dryer exit, so that the easy and precise measurement of this temperature can be the starting point of the feed-back control chain.

2. Materials and Methods

2.1. Mathematical Analysis of the Drying Rate Along the Belt Dryer

Figure 2 [63] represents the scheme of a conveyor-belt dryer with tangential flow completed by the diagram of the temperatures of the air T_A and the product T_P. This one, T_P, was assumed to be equal to the wet bulb temperature T_{WB}.

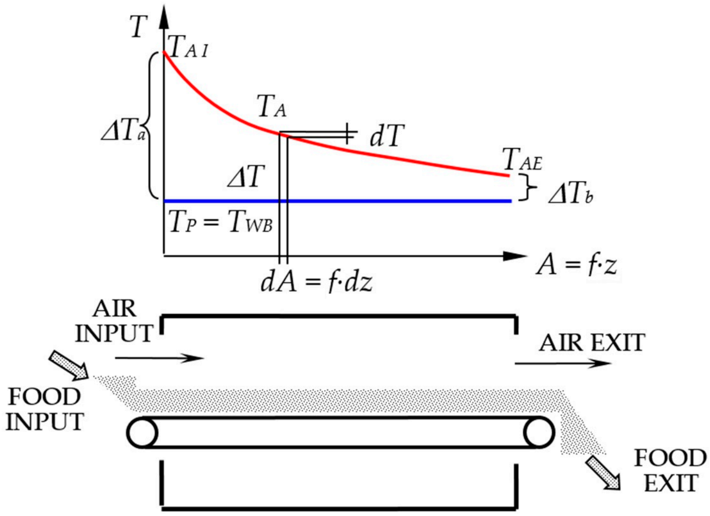

Figure 2. The conveyor-belt dryer with tangential flow and diagram of the temperature of the air and product with a final moisture content $X_F > X_C$.

The infinitesimal heat transfer rate dq, transmitted from the air [64–66] to the product through the infinitesimal area dA, as shown in Figure 2, can be written as follows: $dq = \alpha \cdot dA \cdot (T_A - T_{WB})$; where: α is the convective heat transfer coefficient; dA is the infinitesimal area; T_A is the air temperature when it comes into contact with the area dA; T_{WB} is the product temperature, assumed to be equal to the wet bulb temperature of the air.

Assuming the adiabatic dryer, this infinitesimal heat transfer rate dq is equal to the released one by the dry component of the air when it flows over the infinitesimal area dA, which therefore lowers its temperature by an infinitesimal quantity dT_A: $dq = -G_{AI} \cdot c_A \cdot dT_A$; where: G_{AI} is the mass flow rate of dry air coinciding with the mass flow rate of hot air entering the dryer; c_A is the specific heat of dry air; dA is the infinitesimal area; dT_A is the infinitesimal variation of the air temperature when it touches the area dA. In the conveyor-belt dryer, the drying process takes place along the direction of the belt, i.e., following a variable called z linked to the area A by the relation derived from (18) of the previous work [63]: $A = f \cdot z$; therefore for an infinitesimal length dz, we have: $dA = f \cdot dz$ (Figure 3).

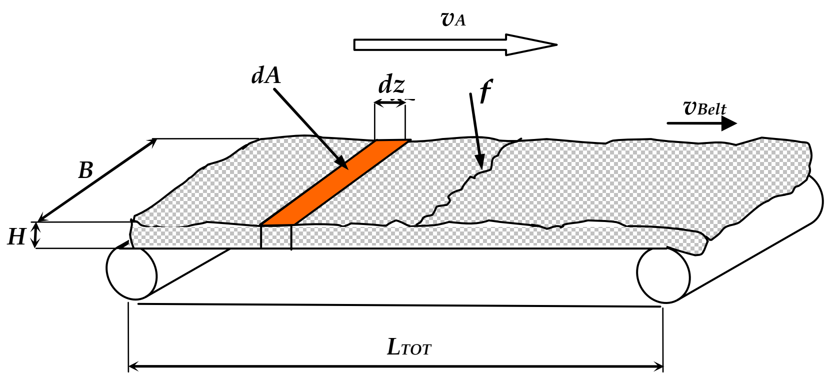

Figure 3. Conveyor-belt dryer with tangential flow in co-current: transverse dimension f; velocity of the drying air v_A; velocity of the belt v_{Belt}; length of the belt L_{TOT}; height of the product bed H; width of the product bed B; infinitesimal area of the product exposed to the air dA; infinitesimal length dz.

By equating the quantities dq, the first ordinary differential equation ODE is obtained:

$$\frac{dT_A}{dz} = -\frac{\alpha \cdot f}{G_{AI} \cdot c_A} \cdot (T_A - T_{WB}) \tag{1}$$

Figure 2 shows that the initial temperature of the product T_{PI} is already equal to the wet bulb temperature T_{WB}. In the enthalpy balance of the dryer [55] the thermal energy required to heat the dry mass of product from T_{PI} to T_{WB} is less than 1% of the total thermal energy supplied by the hot air and the thermal energy required to heat, from T_{PI} to T_{WB}, the water in the product is about 3%. This latter thermal energy was however accounted during the development of the mathematical model [63]. Therefore, the T_{PI} = T_{WB} assumption was acceptable.

The indefinite integral of Equation (1) is easily obtained by separation of variables: $-\frac{\alpha \cdot f \cdot z}{G_{AI} \cdot c_A} = \ln(T_A - T_{WB}) + C$. The integration constant C is obtained with the initial condition of the conveyor-belt dryer: for $z = 0$, $T_A = T_{AI}$; where T_{AI} is the air temperature at the input of the dryer. Therefore: $C = -\ln(T_{AI} - T_{WB})$ and the solution is:

$$(T_A - T_{WB}) = (T_{AI} - T_{WB}) \cdot e^{-\frac{\alpha \cdot f \cdot z}{G_{AI} \cdot c_A}} \quad (2)$$

The presence of the exponential function with the negative exponent and containing the variable z along the conveyor-belt, informs that the air temperature T_A tends asymptotically to the wet bulb temperature. In other words, the thermo-hygrometric equilibrium between air and product, always considered with moisture higher than the critical one, can only be obtained by reaching a length $z = \infty$.

Since in the conveyor-belt dryer with tangential flow the process takes place along the variable z, it is preferable to define the drying rate at point z of the dryer as an alternative of the instantaneous drying rate.

Therefore, at a point located at a distance z from the start of the dryer, an infinitesimal area dA is identified and exposed to the drying air, belonging of an infinitesimal mass of product dm, whose dry component will be dm_D (Figure 3). Therefore the drying rate R [63] at the point at distance z from the start of the dryer becomes: $R = \frac{dG_{EV}}{dm_D}$, since the infinitesimal dry mass dm_D results moistened with water which evaporates with an infinitesimal flow rate dG_{EV}.

The previous equation: $dq = \alpha \cdot dA \cdot (T_A - T_{WB}) = \alpha \cdot f \cdot dz \cdot (T_A - T_{WB})$, informs that an infinitesimal heat transfer rate dq passes from dry air to the product through the infinitesimal area dA. This heat transfer rate dq produces the evaporation of an infinitesimal mass flow rate of water dG_{EV} such that: $dG_{EV} = \frac{dq}{r} = \frac{f \cdot dz \cdot \alpha}{r} \cdot (T_A - T_{WB})$. Where r is the thermal energy to produce 1 kg of superheated water vapor at the air temperature T_A [63]. By inserting this relation in the previous definition of drying rate at the generic point z, we obtain:

$$R = \frac{dG_{EV}}{dm_D} = \frac{f \cdot dz \cdot \alpha}{r \cdot dm_D} \cdot (T_A - T_{WB}) \quad (3)$$

The infinitesimal dry mass dm_D is equal to the difference between the total infinitesimal mass dm of the product and the infinitesimal mass of the water contained in it dm_W: $dm_D = dm - dm_W$. At the initial point of the dryer, both the infinitesimal mass of the product dm_I and the infinitesimal mass of the water dm_{WI} are known, therefore: $dm_D = dm_I - dm_{WI}$.

The moisture content of the product in the initial point of the dryer is also known: $X_I = dm_{WI}/dm_D$; as well as its initial volume dV_I and its initial bulk density: $\rho_{BulkI} = dm_I/dV_I$. Introducing these expressions in the previous one, we have: $dm_D = \rho_{BulkI} \cdot dV_I - dm_D \cdot X_I$. If dm_D is highlighted, we get: $dm_D = \frac{\rho_{BulkI} \cdot dV_I}{1+X_I}$.

Since dV_I is the infinitesimal volume of bulk product which is at the beginning of the conveyor-belt (Figure 3) and which exposes the infinitesimal area dA to the drying air, then this infinitesimal bulk product, wide B_I, high H_I, and long dz, has a volume $dV_I = B_I \cdot H_I \cdot dz$. The infinitesimal dry mass dm_D is: $dm_D = \frac{\rho_{BulkI} \cdot B_I H_I \cdot dz}{1+X_I}$.

Finally, we get:

$$R = \frac{dG_{EV}}{dm_D} = \frac{\alpha \cdot f}{r \cdot \rho_{BulkI} \cdot B_I \cdot H_I} \cdot (1 + X_I)(T_A - T_{WB}) \quad (4)$$

The drying rate R of (4) is the one corresponding to the point at the distance z from the inlet of the dryer (Figure 2) where the air temperature is T_A. Hence, starting from its general definition [63]: $R = \frac{dX}{dt}$; where X is the moisture content on a dry basis, we can write:

$$R = -\frac{dX}{dt} = -\frac{dX}{dz}\cdot\frac{dz}{dt} = -\frac{dX}{dz}\cdot v_{Belt} \tag{5}$$

where the ratio between the infinitesimal length dz and the infinitesimal time interval is the product speed, v_{Belt}. Taking into account (2) and (5), (4) becomes:

$$\frac{dX}{dz} = -\frac{\alpha\cdot f}{v_{Belt}\cdot r\cdot \rho_{BulkI}\cdot B_I\cdot H_I}\cdot(1+X_I)(T_{AI}-T_{WB})\cdot e^{-\frac{\alpha\cdot f\cdot z}{G_{AI}\cdot c_A}} \tag{6}$$

Now, the integration is easy, since: f, v_{Belt}, X_I, ρ_{BulkI}, α, $(T_{AI} - T_{WB})$, r, B_I, H_I, G_{AI}, and c_A, are considered constant [63]. In particular, the transverse dimension f (Figure 3) is an average value over the entire length of the dryer and B_I and H_I are the values of the base and the height of the bulk product at the beginning of the conveyor-belt:

$$X = \frac{\alpha\cdot f\cdot(1+X_I)}{v_{Belt}\cdot r\cdot \rho_{BulkI}\cdot B_I\cdot H_I}\cdot(T_{AI}-T_{WB})\cdot\frac{G_{AI}\cdot c_A}{\alpha\cdot f}\cdot e^{-\frac{\alpha\cdot f\cdot z}{G_{AI}\cdot c_A}} + C$$

The integration constant C is calculated by imposing the final equilibrium conditions: for $z = \infty$, then the moisture content of the product is equal to the equilibrium one, $X = X_{eq}$. We obtain:

$$X - X_{eq} = \frac{\alpha\cdot f\cdot(1+X_I)}{v_{Belt}\cdot r\cdot \rho_{BulkI}\cdot B_I\cdot H_I}\cdot(T_{AI}-T_{WB})\cdot\frac{G_{AI}\cdot c_A}{\alpha\cdot f}\cdot e^{-\frac{\alpha\cdot f\cdot z}{G_{AI}\cdot c_A}} \tag{7}$$

By dividing Equation (7) with Equation (6), we get:

$$\frac{dX}{dz} = -\frac{\alpha\cdot f}{G_{AI}\cdot c_A}\cdot(X_A - X_{eq}) \tag{8}$$

which indicates that it is an ordinary first-order differential equation. This is the second ODE of the mathematical analysis of drying. Its existence was easily predicted since the moisture content of the product X and its derivative dX/dz is both a function of the length z means through an exponential function (Figure 4).

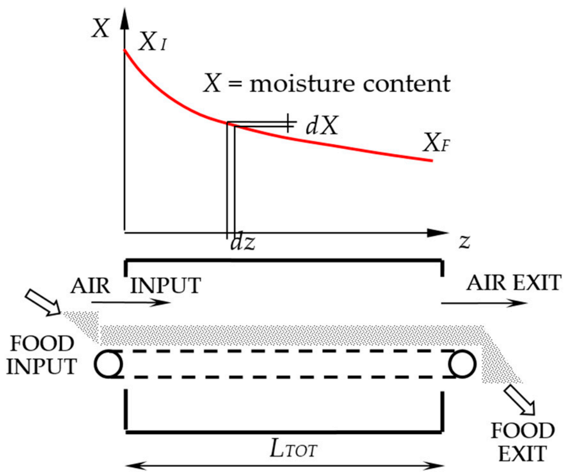

Figure 4. Conveyor-belt dryer with tangential flow completed with the moisture content product diagram.

This Ordinary Differential Equation (8), after integration, can be a useful tool for the design and adjustment of the dryer. However, it needs the exact value of the equilibrium moisture content *Xeq*. Since this last depends both on the nature of the product and on the temperature and humidity of the drying air at the end of the dryer, its evaluation is very complicated.

To overcome the obstacle of equilibrium moisture content, the Equation (6) can be integrated by imposing the initial conditions of the dryer: for $z = 0$, the moisture content of the product is $X = X_I$. We get:

$$X - X_I = \frac{G_{AI} \cdot c_A \cdot (1 + X_I)}{v_{Belt} \cdot r \cdot \rho_{BulkI} \cdot B_I \cdot H_I} \cdot (T_{AI} - T_{WB}) \cdot \left[1 - e^{-\frac{\alpha \cdot f \cdot z}{G_{AI} \cdot c_A}}\right] \tag{9}$$

Introducing the Equation (2) as the solution of Ordinary Differential Equation (1), into Equation (9) and setting $z = L_{TOT}$, we obtain:

$$X_F = X_I + \frac{G_{AI} \cdot c_A \cdot (1 + X_I)}{v_{Belt} \cdot r \cdot \rho_{BulkI} \cdot B_I \cdot H_I} \cdot (T_{AE} - T_{AI}) \tag{10}$$

which gives the value of the final moisture content of the product X_F as a function of the air temperature at the exit of the dryer T_{AE}.

2.2. Adjustment of Parameters of the Dryer

Previously, with a mathematical modeling [63] an Equation (25) was obtained which correlated the final moisture content of the product X_F to some operating parameters of the non-perforated belt dryer, in particular the speed of the belt v_{Belt} and the inlet temperature of the hot air T_{AI}. Therefore, that Equation (25) can be used to design a dryer regulation system such as to ensure a constant value of the final moisture content X_F, avoiding the risks of products that are not very dry and therefore perishable, or that are too dry with a waste of energy.

The weakness of this adjustment system was, and continues to be, the experimental in-line measurement of final moisture content X_F at the dryer exit. These are always indirect measurements which use, for example, the dielectric properties of the dried product. The result is not always accurate because the composition of the dry matter also affects the dielectric properties. Furthermore, the measurement must be performed quickly to allow the adjustment system to intervene promptly and this leads to an unacceptable increase in the cost of the online hygrometer.

To overcome these difficulties, Equation (10) can be used to determine the final moisture content X_F through the easy, accurate, and immediate measurement of the air exit temperature T_{AE}.

The measurement of the air inlet temperature T_{AI} is also easy, precise, and immediate, while the measurement of the inlet moisture content X_I can be carried out without haste and with precision in the laboratory by sampling the wet product before being fed to the dryer.

2.3. Experimental Equipment

A pilot drying plant (Figure 5) as used to verify the validity of Equation (10). It was the same used for the validation of the mathematical model proposed in the previous work [63]. In this case alfalfa was also used as a vegetable product to be dried. Alfalfa was in the form of stems (with leaves) cut and collected immediately from the open field with the stems then cut into pieces 5 cm long. The operating diagram corresponds to that of Figure 1, while the geometric and operational characteristics are shown in Table 1. In the table the value of the product between the form factor F and the convective heat transfer coefficient α is also reported. This product $F \cdot \alpha$ was determined experimentally in the previous work [63]. Besides the form factor F is the ratio of surface of the alfalfa to its volume, i.e., $F = \frac{S}{V} = \frac{f \cdot L_{TOT}}{B_I \cdot H_I \cdot L_{TOT}} = \frac{f}{B_I . H_I}$, where: L_{TOT} is the total length of the belt of the dryer; H_I is the initial height of the product bed; B_I is the initial width of the product; f is the transverse dimension (Figure 3) [63].

Figure 5. Pilot conveyor-belt dryer with tangential flow.

Table 1. Geometrical and some operational data of the pilot dryer.

Quantity	Symbol	Value
Belt width	B_I (m)	0.3
Belt length	L_{TOT} (m)	6.0
Alfalfa bulk height	H_I (m)	0.05
Air section	A_A (m^2)	0.15
Form factor·Convective heat transfer coefficient [63]	$F \cdot \alpha$ (W·m^{-3}·K^{-1})	5144
Transverse dimension (Figure 3)·Convect. heat transf. coeff.	$f \cdot \alpha = B_I \cdot H_I \cdot F \cdot \alpha$ (W·m^{-1}·K^{-1})	77.16
Air mass flow rate [63]	G_{AI} (kg·s^{-1})	0.354
Alfalfa input moisture content (D.B.)	X_I	1.892 ± 0.110
Alfalfa input moisture content (W.B.)	Y_I (%)	65.4 ± 1.3
Alfalfa input bulk density	ρ_{BulkI} (kg·m^{-3})	197 ± 7.5
Thermal energy [63]	r (kJ·kg^{-1})	2617

The materials and methods used were: the PT100 resistance thermometers (Deltaohm HD 2107.1 with probes TP475A.0, Padova, Italy) for the measurement of inlet and outlet temperature of the dryer; the data logger (Deltaohm HD 32.8.16, Padova, Italy) for the registration; the precision balance (Kern & Sohn 440-45N, Balingen, Germany) for the weighing of the sample before and after dehydration in an oven (Memmert UF55, Schwabach, Germany) for two hours at 135 °C regarding the moisture content of the product at the inlet and outlet; the Pitot anemometer for the measurement of the air velocity (Deltaohm HD 2114P.0 with probe T2-400, Padova, Italy). Five replicates were made for each test. Finally the bulk density was calculated after measuring the volume and mass of the samples.

3. Results and Discussion

3.1. Experimental Results

To verify experimentally the Equation (10), two different conveyor-belt speeds and two different air temperatures at the inlet were programmed. The results of the measurement of the mean values of the air temperature at the input T_{AI} and the exit T_{AE} of the dryer, completed by the relative standard deviations (S.D.), are shown in the Table 2. In addition, the Table 2 shows the mean value and the S.D. of the alfalfa final moisture content at the exit of the dryer.

Table 2. Experimental data of the pilot dryer.

Belt Speed	Air Input Velocity	Air Input Temperature	Air Exit Temperature	Alfalfa Exit Moisture Cont.
v_{Belt} (m/s)	v_{AI} (m/s)	$T_{AI} \pm$ S.D. (°C)	$T_{AE} \pm$ S.D. (°C)	$X_F \pm$ S.D.
0.005	2.6	119.2 ± 1.3	58.3 ± 1.2	0.332 ± 0.016
0.005	2.5	99.5 ± 1.1	51.8 ± 0.9	0.667 ± 0.023
0.006	2.6	119.2 ± 1.3	59.1 ± 1.1	0.607 ± 0.022
0.006	2.5	99.5 ± 1.1	52.2 ± 0.9	0.879 ± 0.025

The speed of the air at the inlet to the dryer was also measured. Table 2 shows a slight difference (only 0.1 m/s) based on the values of the air temperature at the inlet. In fact, the air was produced by a fan placed before the heater. Therefore, its mass flow rate G_{AI} was independent of the air temperature at the input of the dryer, but the air speed v_{AI} was instead different as the air density was different. At this point there could be a risk that the two different values of v_{AI} could affect the convection coefficient α and therefore affect $F{\cdot}\alpha$. The measurements made on $F{\cdot}\alpha$ during the tests described in [63] have however shown that $F{\cdot}\alpha$ does not differ significantly between the two cases.

3.2. Discussion

The comparison between the experimental values of the final moisture content of alfalfa and those calculated with (10) is shown in Table 3. The relative error is not negligible, especially for the low values of the moisture content. These errors can be explained using the same (10) to highlight the heat flow provided by the hot air, $G_{AI}{\cdot}c_A \cdot (T_{AI} - T_{AE})$ and that required by the water to evaporate, $v_{Belt}{\cdot}r{\cdot}\rho_{BulkI}{\cdot}B_I{\cdot}H_I{\cdot}\frac{(X_I - X_F)}{(1+X_I)}$:

$$G_{AI}{\cdot}c_A \cdot (T_{AI} - T_{AE}) = v_{Belt}{\cdot}r{\cdot}\rho_{BulkI}{\cdot}B_I{\cdot}H_I{\cdot}\frac{(X_I - X_F)}{(1 + X_I)} \tag{11}$$

Table 3. Alfalfa experimental moisture content values at the exit dryer vs. calculated ones by Equation (10).

Belt Speed	Air Input Temperature	Air Exit Temperature	Experimental Alfalfa Exit Moisture Cont.	Calculated Alfalfa Exit Moisture Cont.	Relat. Error
v_{Belt} (m/s)	T_{AI} (°C)	T_{AE} (°C)	X_F	X_F	(%)
0.005	119.2	58.3	0.332	0.272	18.1
0.005	99.5	51.8	0.667	0.623	6.6
0.006	119.2	59.1	0.607	0.559	7.9
0.006	99.5	52.2	0.879	0.843	4.1

Obviously, Equation (11) is satisfied with the values of X_F calculated with (10), but it is no longer satisfied if we introduce the experimental values of Table 3. In Table 4 the absolute differences Δ (W) and the percentage differences δ (%) between the heat transfer rate provided by the air and the used one by the water to evaporate are reported. The percentage differences appear practically constant with an average value $\delta_m = -3.54\%$.

Table 4. Comparison between the heat transfer rate from hot air and the heat transfer rate to produce superheated steam at temperature of the air T_A.

v_{Belt} (m/s)	T_{AI} (°C)	T_{AE} (°C)	$G_{AI}c_A(T_{AI}-T_{AE})$	$v_{Belt}r\rho_{BulkI}B_IH_I\frac{(X_I-X_F)}{(1+X_I)}$	Δ (W)	δ (%)
0.005	119.2	58.3	21,666	20,857	−809	−3.73
0.005	99.5	51.8	16,970	16,378	−592	−3.48
0.006	119.2	59.1	21,382	20,631	−751	−3.51
0.006	99.5	52.2	16,828	16,253	−575	−3.42

On the other hand, the mathematical development both in the previous work [63] and in this one, was made by hypotheses that the dryer was adiabatic and the thermal energy necessary to heat the dry mass of product from T_{PI} to T_{WB} was small compared to thermal energy r, (less than 1%), and therefore negligible.

These simplifying hypotheses lead to predictions of final moisture content X_F with acceptable errors for high X_F expected values, but the errors become unacceptable with low expected X_F (Table 3), however above the critical value.

In any case the introduction in Equation (10) of a corrective coefficient equal to $\eta = \left(1 - \frac{|\delta_m|}{100}\right)$ multiplying the temperature difference $(T_{AI} - T_{AE})$, was possible:

$$X_F = X_I + \frac{G_{AI}\cdot c_A\cdot(1+X_I)}{v_{Belt}\cdot r\cdot \rho_{BulkI}\cdot B_I\cdot H_I}\cdot(T_{AE} - T_{AI})\cdot\eta \quad (12)$$

In this manner the heat losses from the walls of the dryer and the heat necessary to raise the temperature of the dry matter from T_{PI} to T_{WB}, was considered. For the pilot dryer, the corrective coefficient is: $\eta = \left(1 - \frac{3.54}{100}\right) = 0.9646$. Therefore, Equation (12) provides the new calculated X_F values corrected as in Table 5, where the errors with respect to the experimental values are also reported. Errors are now negligible.

Table 5. Alfalfa experimental moisture content values at the exit dryer vs. calculated ones by Equation (12).

Belt Speed	Air Input Temperature	Air Exit Temperature	Experimental Alfalfa Exit Moisture Cont.	Calculated Alfalfa Exit Moisture Cont.	Relat. Error
v_{Belt} (m/s)	T_{AI} (°C)	T_{AE} (°C)	X_F	X_F	(%)
0.005	119.2	58.3	0.332	0.329	0.9
0.005	99.5	51.8	0.667	0.668	0.09
0.006	119.2	59.1	0.607	0.606	0.13
0.006	99.5	52.2	0.879	0.880	0.11

4. Conclusions

In industrial dryers a feedback control system is often present. So, a chain of control, starting with an instant measurement of the final moisture of the X_F product, is necessary. Direct measurement by weighing the moisture content cannot be done instantly. For instantaneous measurement it is necessary to use, for example, the dielectric/capacitive properties of the product, but expensive instruments based on the measurement of the dielectric properties of the product are not always accurate because of the high product flow rate.

For this reason, in this work a mathematical analysis to develop two ordinary differential equations (ODEs) was made, specifically for drying in the conveyor-belt dryer with tangential flow with final moisture content of the product X_F higher than the critical value X_C. The solution of the ODEs has become an Equation (10) between various quantities including: the moisture content of the initial X_I and final X_F product and the initial T_{AI} and final T_{AE} air temperatures. However, the ODEs were obtained by imposing the absence of heat losses from the wall of the dryer and the initial temperature of the entering product equal to the wet bulb temperature. Because of this initial hypothesis, the comparison between the results obtained with Equation (10) and the experimental ones showed too high an error when the final moisture content of the product is low. By analysis of the results of comparison, it was calculated that the sum of the waste heat and the heat necessary to raise the temperature of the product up to the wet bulb temperature corresponds to a practically constant δ_m = 3.54% with respect to the total heat supplied with the hot air. Then a corrective coefficient equal to $\eta = \left(1 - \frac{|\delta_m|}{100}\right)$ was introduced in Equation (10), so that the obtained Equation (12) always presents negligible errors with respect to the experimental data. Therefore, Equation (12) is a relationship between the final moisture content of the product and the air temperature at the exit of the dryer, so by measuring the latter and using the Equation (12) we have a quick and precise value of X_F as starting data of the feed-back control chain.

Finally, an expansion of the mathematical modeling for the case of the final product moisture content lower than the critical one ($X_F < X_C$) is also necessary in a further future work.

Funding: This research received no external funding.

Institutional Review Board Statement: Not applicable.

Informed Consent Statement: Not applicable.

Data Availability Statement: The data presented in this study is contained within the article.

Conflicts of Interest: The author declares no conflict of interest.

References

1. Omolola, A.O.; Jideani, A.I.O.; Kapila, P.F. Quality properties of fruits as affected by drying operation. *Crit. Rev. Food Sci. Nutr.* **2017**, *57*, 95–108. [CrossRef]
2. Caccavale, P.; De Bonis, M.V.; Ruocco, G. Conjugate heat and mass transfer in drying: A modeling review. *J. Food Eng.* **2016**, *176*, 28–35. [CrossRef]
3. Fernandes, F.A.N.; Rodrigues, S.; Law, C.L.; Mujumdar, A.S. Drying of exotic tropical fruits: A comprehensive review. *Food Bioprocess Technol.* **2011**, *4*, 163–185. [CrossRef]
4. Kaleta, A.; Gornicki, K.; Winiczenko, R.; Chojnacka, A. Evaluation of drying models of apple (var. Ligol) dried in a fluidized bed dryer. *Energy Convers. Manag.* **2013**, *67*, 179–185. [CrossRef]
5. Marquez, C.A.; de Michelis, A. Comparison of drying kinetics for small fruits with and without particle shrinkage considerations. *Food Bioprocess Technol.* **2011**, *4*, 1212–1218. [CrossRef]
6. Tzempelikos, D.A.; Mitrakos, D.; Vouros, A.P.; Bardakas, A.V.; Filios, A.E.; Margaris, D.P. Numerical modeling of heat and mass transfer during convective drying of cylindrical quince slices. *J. Food Eng.* **2015**, *156*, 10–21. [CrossRef]
7. Bezerra, C.V.; Meller Da Silva, L.H.; Correa, D.F.; Rodrigues, A.M.C. A modeling study for moisture diffusivities and moisture transfer coefficients in drying of passion fruit peel. *Int. J. Heat Mass Tran.* **2015**, *85*, 750–755. [CrossRef]
8. García-Alvarado, M.A.; Pacheco-Aguirre, F.M.; Ruiz-Lopez, I.I. Analytical solution of simultaneous heat and mass transfer equations during food drying. *J. Food Eng.* **2014**, *142*, 39–45. [CrossRef]
9. Ertekin, C.; Firat, M.Z. A comprehensive review of thin layer drying models used in agricultural products. *Crit. Rev. Food Sci. Nutr.* **2017**, *57*, 701–717. [CrossRef]
10. Fernando, W.J.N.; Low, H.C.; Ahmad, A.L. Dependence of the effective diffusion coefficient of moisture with thickness and temperature in convective drying of sliced materials. A study on slices of banana, cassava and pumpkin. *J. Food Eng.* **2011**, *102*, 310–316. [CrossRef]
11. Friso, D. A Mathematical Solution for Food Thermal Process Design. *Appl. Math. Sci.* **2015**, *9*, 255–270. [CrossRef]
12. Friso, D.; Baldoin, C. Mathematical Modelling and Experimental Assessment of Agrochemical Drift using a Wind Tunnel. *Appl. Math. Sci.* **2015**, *9*, 5451–5463. [CrossRef]
13. Friso, D. An Approximate Analytic Solution to a Non-Linear ODE for Air Jet Velocity Decay through Tree Crops Using Piecewise Linear Emulations and Rectangle Functions. *Appl. Sci.* **2019**, *9*, 5440. [CrossRef]
14. Akdas, S.; Baslar, M. Dehydration and degradation kinetics of bioactive compounds for mandarin slices under vacuum and oven drying conditions. *J. Food Process. Preserv.* **2015**, *39*, 1098–1107. [CrossRef]
15. Askari, G.R.; Emam-Djomeh, Z.; Mousavi, S.M. Heat and mass transfer in apple cubes in a microwave-assisted fluidized bed drier. *Food Bioprod. Process.* **2013**, *91*, 207–215. [CrossRef]
16. Ben Mabrouk, S.; Benali, E.; Oueslati, H. Experimental study and numerical modelling of drying characteristics of apple slices. *Food Bioprod. Process.* **2012**, *90*, 719–728. [CrossRef]

17. Esfahani, J.A.; Vahidhosseini, S.M.; Barati, E. Three-dimensional analytical solution for transport problem during convection drying using Green's function method (GFM). *Appl. Therm. Eng.* **2015**, *85*, 264–277. [CrossRef]
18. Esfahani, J.A.; Majdi, H.; Barati, E. Analytical two-dimensional analysis of the transport phenomena occurring during convective drying: Apple slices. *J. Food Eng.* **2014**, *123*, 87–93. [CrossRef]
19. Golestani, R.; Raisi, A.; Aroujalian, A. Mathematical modeling on air drying of apples considering shrinkage and variable diffusion coefficient. *Dry. Technol.* **2013**, *31*, 40–51. [CrossRef]
20. Bon, J.; Rossellò, C.; Femenia, A.; Eim, V.; Simal, S. Mathematical modeling of drying kinetics for Apricots: Influence of the external resistance to mass transfer. *Dry. Technol.* **2007**, *25*, 1829–1835. [CrossRef]
21. Barati, E.; Esfahani, J.A. A new solution approach for simultaneous heat and mass transfer during convective drying of mango. *J. Food Eng.* **2011**, *102*, 302–309. [CrossRef]
22. Corzo, O.; Bracho, N.; Alvarez, C.; Rivas, V.; Rojas, Y. Determining the moisture transfer parameters during the air-drying of mango slices using biot-dincer numbers correlation. *J. Food Process. Eng.* **2008**, *31*, 853–873. [CrossRef]
23. Janjai, S.; Lamlert, N.; Intawee, P.; Mahayothee, B.; Haewsungcharern, M.; Bala, B.K.; Müller, J. Finite element simulation of drying of mango. *Biosyst. Eng.* **2008**, *99*, 523–531. [CrossRef]
24. Villa-Corrales, L.; Flores-Prieto, J.J.; Xamàn-Villasenor, J.P.; García-Hernàndez, E. Numerical and experimental analysis of heat and moisture transfer during drying of Ataulfo mango. *J. Food Eng.* **2010**, *98*, 198–206. [CrossRef]
25. Corzo, O.; Bracho, N.; Pereira, A.; Vàsquez, A. Application of correlation between Biot and Dincer numbers for determining moisture transfer parameters during the air drying of coroba slices. *J. Food Process. Preserv.* **2009**, *33*, 340–355. [CrossRef]
26. Guiné, R.P. Pear drying: Experimental validation of a mathematical prediction model. *Food Bioprod. Process.* **2008**, *86*, 248–253. [CrossRef]
27. Kaya, A.; Aydin, O.; Dincer, I. Experimental and numerical investigation of heat and mass transfer during drying of Hayward kiwi fruits (Actinidia Deliciosa Planch). *J. Food Eng.* **2008**, *88*, 323–330. [CrossRef]
28. Lemus-Mondaca, R.A.; Zambra, C.E.; Vega-Gàlvez, A.; Moraga, N.O. Coupled 3D heat and mass transfer model for numerical analysis of drying process in papaya slices. *J. Food Eng.* **2013**, *116*, 109–117. [CrossRef]
29. Ramsaroop, R.; Persad, P. Determination of the heat transfer coefficient and thermal conductivity for coconut kernels using an inverse method with a developed hemispherical shell model. *J. Food Eng.* **2012**, *110*, 141–157. [CrossRef]
30. Sabarez, H.T. Mathematical modeling of the coupled transport phenomena and color development: Finish drying of trellis-dried sultanas. *Dry. Technol.* **2014**, *32*, 578–589. [CrossRef]
31. Baini, R.; Langrish, T.A.G. Choosing an appropriate drying model for intermittent and continuous drying of bananas. *J. Food Eng.* **2007**, *79*, 330–343. [CrossRef]
32. Da Silva, W.P.; Silva, C.M.D.P.S.; Gomes, J.P. Drying description of cylindrical pieces of bananas in different temperatures using diffusion models. *J. Food Eng.* **2013**, *117*, 417–424. [CrossRef]
33. Da Silva, W.P.; Hamawand, I.; Silva, C.M.D.P.S. A liquid diffusion model to describe drying of whole bananas using boundary-fitted coordinates. *J. Food Eng.* **2014**, *137*, 32–38. [CrossRef]
34. Castro, A.M.; Mayorga, E.Y.; Moreno, F.L. Mathematical modelling of convective drying of fruits: A review. *J. Food Eng.* **2018**, *223*, 152–167. [CrossRef]
35. Chandra Mohan, V.P.; Talukdar, P. Three dimensional numerical modeling of simultaneous heat and moisture transfer in a moist object subjected to convective drying. *Int. J. Heat Mass Tran.* **2010**, *53*, 4638–4650. [CrossRef]
36. Defraeye, T. When to stop drying fruit: Insights from hygrothermal modelling. *Appl. Therm. Eng.* **2017**, *110*, 1128–1136. [CrossRef]
37. Defraeye, T.; Radu, A. International Journal of Heat and Mass Transfer Convective drying of fruit: A deeper look at the air-material interface by conjugate modeling. *Int. J. Heat Mass Tran.* **2017**, *108*, 1610–1622. [CrossRef]
38. Fanta, S.W.; Abera, M.K.; Ho, Q.T.; Verboven, P.; Carmeliet, J.; Nicolai, B.M. Microscale modeling of water transport in fruit tissue. *J. Food Eng.* **2013**, *118*, 229–237. [CrossRef]
39. Da Silva, W.P.; e Silva, C.M.; e Silva, D.D.; de Araújo Neves, G.; de Lima, A.G. Mass and heat transfer study in solids of revolution via numerical simulations using finite volume method and generalized coordinates for the Cauchy boundary condition. *Int. J. Heat Mass Tran.* **2010**, *53*, 1183–1194. [CrossRef]
40. Aversa, M.; Curcio, S.; Calabro, V.; Iorio, G. An analysis of the transport phenomena occurring during food drying process. *J. Food Eng.* **2007**, *78*, 922–932. [CrossRef]
41. Da Silva, W.P.; Precker, J.W.; e Silva, D.D.; e Silva, C.D.; de Lima, A.G. Numerical simulation of diffusive processes in solids of revolution via the finite volume method and generalized coordinates. *Int. J. Heat Mass Tran.* **2009**, *52*, 4976–4985. [CrossRef]
42. Datta, A.K. Porous media approaches to studying simultaneous heat and mass transfer in food processes. I: Problem formulations. *J. Food Eng.* **2007**, *80*, 80–95. [CrossRef]
43. Defraeye, T. Advanced computational modelling for drying processes—A review. *Appl. Energy* **2014**, *131*, 323–344. [CrossRef]
44. Defraeye, T.; Verboven, P.; Nicolai, B. CFD modelling of flow and scalar exchange of spherical food products: Turbulence and boundary-layer modelling. *J. Food Eng.* **2013**, *114*, 495–504. [CrossRef]
45. Erbay, Z.; Icier, F. A review of thin layer drying of foods: Theory, modeling, and experimental results. *Crit. Rev. Food Sci. Nutr.* **2010**, *50*, 441–464. [CrossRef]
46. Giner, S.A. Influence of Internal and External Resistances to Mass Transfer on the constant drying rate period in high-moisture foods. *Biosyst. Eng.* **2009**, *102*, 90–94. [CrossRef]

47. Khan, F.A.; Straatman, A.G. A conjugate fluid-porous approach to convective heat and mass transfer with application to produce drying. *J. Food Eng.* **2016**, *179*, 55–67. [CrossRef]
48. Lamnatou, C.; Papanicolaou, E.; Belessiotis, V.; Kyriakis, N. Conjugate heat and mass transfer from a drying rectangular cylinder in confined air flow. *Numer. Heat Tran.* **2009**, *56*, 379–405. [CrossRef]
49. Oztop, H.F.; Akpinar, E.K. Numerical and experimental analysis of moisture transfer for convective drying of some products. *Int. Commun. Heat Mass Tran.* **2008**, *35*, 169–177. [CrossRef]
50. Ruiz-Lòpez, I.I.; García-Alvarado, M.A. Analytical solution for food-drying kinetics considering shrinkage and variable diffusivity. *J. Food Eng.* **2007**, *79*, 208–216. [CrossRef]
51. Vahidhosseini, S.M.; Barati, E.; Esfahani, J.A. Green's function method (GFM) and mathematical solution for coupled equations of transport problem during convective drying. *J. Food Eng.* **2016**, *187*, 24–36. [CrossRef]
52. Van Boekel, M.A.J.S. Kinetic modeling of food quality: A critical review. *Compr. Rev. Food Sci. Food Saf.* **2008**, *7*, 144–158. [CrossRef]
53. Wang, W.; Chen, G.; Mujumdar, A.S. Physical interpretation of solids drying: An overview on mathematical modeling research. *Dry. Technol.* **2007**, *25*, 659–668. [CrossRef]
54. Friso, D. *Ingegneria Dell'industria Agroalimentare (Food Engineering Operations)*, 1st ed.; CLEUP: Padova, Italy, 2018; Volume 2, pp. 98–105.
55. Geankoplis, C.J. *Transport Process Unit Operations*, 3rd ed.; Prentice-Hall International: Englewood Cliffs, NJ, USA, 1993; pp. 520–562.
56. Salemović, D.R.; Dedić, A.D.; Ćuprić, N.L. Two-dimensional mathematical model for simulation of the drying process of thick layers of natural materials in a conveyor-belt dryer. *Therm. Sci.* **2017**, *21*, 1369–1378. [CrossRef]
57. Salemović, D.R.; Dedić, A.D.; Ćuprić, N.L. A mathematical model and simulation of the drying process of thin layers of potatoes in a conveyor-belt dryer. *Therm. Sci.* **2015**, *19*, 1107–1118. [CrossRef]
58. Xanthopoulos, G.; Okoinomou, N.; Lambrinos, G. Applicability of a single-layer drying model to predict the drying rate of whole figs. *J. Food Eng.* **2017**, *81*, 553–559. [CrossRef]
59. Khankari, K.K.; Patankar, S.V. Performance analysis of a double-deck conveyor dryer—A computational approach. *Dry. Technol.* **1999**, *17*, 2055–2067. [CrossRef]
60. Kiranoudis, C.T.; Maroulis, Z.B.; Marinos-Kouris, D. Dynamic Simulation and Control of Conveyor-Belt Dryers. *Dry. Technol.* **1994**, *12*, 1575–1603. [CrossRef]
61. Pereira de Farias, R.; Deivton, C.S.; de Holanda, P.R.H.; de Lima, A.G.B. Drying of Grains in Conveyor Dryer and Cross Flow: A Numerical Solution Using Finite-Volume Method. *Rev. Bras. Pr. Agroind.* **2004**, *6*, 1–16. [CrossRef]
62. Kiranoudis, C.T.; Markatos, N.C. Pareto design of conveyor-belt dryers. *J. Food Eng.* **2000**, *46*, 145–155. [CrossRef]
63. Friso, D. Conveyor-belt dryers with tangential flow for food drying: Mathematical modeling and design guidelines for final moisture content higher than the critical value. *Inventions* **2020**, *5*, 22. [CrossRef]
64. Friso, D.; Bortolini, L.; Tono, F. Exergetic analysis and exergy loss reduction in the milk pasteurization for Italian cheese production. *Energies* **2020**, *13*, 750. [CrossRef]
65. Friso, D. Energy saving with total energy system for cold storage in Italy: Mathematical modeling and simulation, exergetic and economic analysis. *Appl. Math. Sci.* **2014**, *8*, 6529–6546. [CrossRef]
66. Cerruto, E.; Balsari, P.; Oggero, G.; Friso, D.; Guarella, A.; Raffaelli, M. Operator safety during pesticide application in greenhouses: A survey on Italian situation. *Acta Hortic.* **2008**, *801*, 1507–1514. [CrossRef]